**Bulletin of Electrical Engineering and Informatics**
Vol. 13, No. 5, October 2024, pp. 3001~3012
ISSN: 2302-9285, DOI: 10.11591/eei.v13i5.7508 

# Design and analysis of sustainable photovoltaic solar charging system with battery storage for electric vehicles

**Eyad Radwan[1], Emad Awada[2], Mutasim Nour[3]**
[1]Department of Electrical Engineering, Faculty of Engineering and Technology, Applied Science Private University, Amman, Jordan
[2]Department of Electrical Engineering, Faculty of Engineering Technology, Al-Balqa Applied University, Amman, Jordan
[3]School of Engineering and Physical Sciences, Heriot-Watt University, Dubai, United Arab Emirates

**Article Info**

***Article history:***

Received Sep 3, 2023
Revised Feb 17, 2024
Accepted Mar 20, 2024

***Keywords:***

DC converter
Electric vehicles
Perturb and observe
Photovoltaic car park
Proportional integral controllers

**ABSTRACT**

This paper presents a sustainable electric vehicle (EV) charging system that operates in three modes of operation to maximize the yield of photovoltaic (PV) system. The design and analysis of the EV charging system is customized based on the operational or office hours of a corporation. The proposed system incorporates a battery pack capable of providing at least one day of autonomy to overcome the weather conditions during early morning, shading times, or cloudy days. In this study, the perturb and observe (P&O) algorithm is modified and used to operate the PV system at maximum power point (MPP) when charging either the EV or the storage battery. The load current, in both cases, is regulated using proportional integral (PI) controllers and pulse width modulation (PWM) switching of DC-DC converter. The proposed system operation is switched between three modes (boost operation for direct charging of EV and discharging of storage battery, and buck operation for charging of storage battery) by a simple event-driven finite state machine (FSM). Simulation results showed excellent tracking behavior of the proposed system when supplying a 5 kW load with variation in solar irradiance between 1000 and 400 W/m$^2$, battery state of charge (SOC) between 40% and 100%, and temperature between 15 to 39 ℃.

*This is an open access article under the CC BY-SA license.*

***Corresponding Author:***

Eyad Radwan
Department of Electrical Engineering, Faculty of Engineering and Technology
Applied Science Private University
Al Arab st. 21-Amman, Jordan
Email: e_redwan@asu.edu.jo

## 1. INTRODUCTION

The last decade witnessed an exponential increase in the production of electric vehicles (EVs) coupled with a rapid increase in the generation of electricity from renewable resources. According to the International Energy Agency (IEA) report over 26 million electric cars were on the road in 2022, up 60% relative to 2021 and more than 5 times the stock in 2018 [1]. At the same time, generation of electricity from renewable energy sources, considering only photovoltaic (PV) and wind, is also growing between 15-20% per annum based on a 10-year average and is predicted to exceed the world annual growth in electricity demand by 2023 [2]. The annual growth in electricity demand is also met by a balancing growth in the amount of energy generated from renewable resources resulting in a reduction in the power sector emissions, which is a favorable environmental impact.

The EV market is expected to grow with its share of electricity consumption predicted to constitute 4% of global electricity demand by 2030 [1]. Therefore, simultaneous investments to expand the existing

power networks and increase their capacities are also necessary. However, considering the economic, environmental, convenience and technical benefits, off grid charging stations present a promising solution to support the expanding EV markets. Off grid charging stations will also contribute to making the low voltage distribution network free from overloading of distribution transformers, overloading of network feeders and avoids various impacts caused by the charging of EVs [3].

Recently, numerous studies have been conducted on topics related to the design, analysis, and sizing of a standalone PV system for various applications, including electrification of remote locations and charging of EVs, while taking into consideration the economic and environmental advantages. Naqvi *et al*. [4] discussed the design of an off-grid PV system for electrification of remote location with emphasis on estimating the battery storage requirements to fulfill the energy demand during the night and cloudy seasons. Similar studies on the number of days of autonomy and the sizing of a standalone PV system for EV charging station applications are presented in [3], [5]–[7].

Integration of renewable energy sources to form modern smart grids and green uninterrupted power supplies to meet the consumer demands while using multiple input converters for combining more than one source of power to supply their energy simultaneously to different types of loads were addressed by many researchers [8]–[11]. However, for most applications involving supplying an individual or a personal need of energy, usually a single source of renewable energy supported with a storge battery is utilized to supply a remote home or a high-power demanding appliance such as an EV [12]–[14]. Such arrangements are finding wide acceptance to maximize the economic and environmental advantages of green and convenient mobility [15]–[21].

Specific designs and topologies for EV chargers were discussed in literature, such as fast DC charger for EVs based on buck converter design without storage, where the charger is supplied by PV modules that used perturb and observe (P&O) method to maximize the output of the PV system in [15]. Genetic algorithm is used by authors in [17] to obtain an optimal sizing of a standalone PV fast charging system to demonstrate the economic viability of such system for EV applications. A comprehensive review of topologies, merits and demerits of multiple input converters is presented in [16]. Converters were divided broadly into three categories: electrically, electromagnetically, and magnetically connected converters based on the type of isolation between the converter input and output ports. On the other hand, Brenna *et al*. [22] discussed the architecture and topologies of EV chargers charging technologies and broadly classified them as on-board chargers and off-board chargers.

In this study, the worst month peak sun hour (PSH) solar irradiance is used to size and design a simple and efficient EV charging system. The proposed system is supplied by PV panels and operates in an off-grid configuration with the support of a storage battery to provide one day of autonomy. The proposed system operates in three independent modes that are determined based on the level of solar irradiance, the existence of EV load, and the state of charge (SOC) of the storage battery. To maximize the efficiency of the system, P&O algorithm is implemented to always operate the PV system at maximum power point (MPP). The switching between the operating modes is managed by a simple event driven finite state machine (FSM). Simple proportional integral (PI) controllers are used to regulate the operation of pulse width modulation (PWM) driven DC-DC converters. The model and design of the proposed system is verified using Simulink from MATLAB.

## 2. METHOD

The block diagram of the proposed charging system is shown in Figure 1. The system consists mainly of PV panels, storage battery, DC-DC converter, and an inverter to provide a standard 230 V (AC plug) to supply any portable EV charger. To simplify the design of the proposed system, The three modes of operation are assumed as follows:

– Mode 1: PV supplying the EV load.

In this mode the main source of energy is the solar PV system, if $P_{pv} > 0.5P_{pv\,rated}$ and the EV load exists, then the source will supply the load (EV system) by triggering a boost convert operation.

– Mode 2: charging the storage battery.

In this mode the main source of energy is the solar PV system, if $P_{pv} > 0.5P_{pv\,rated}$ and the EV load is disconnected, the PV system will charge the storage battery if the $SOC < 90\%$ through a buck converter operation.

– Mode 3: discharging the storage battery.

In this mode the main source of energy is the storage battery, if the battery $SOC > 40\%$, and the EV load exists, the storage battery will supply the load (EV system) by triggering a boost convert operation.

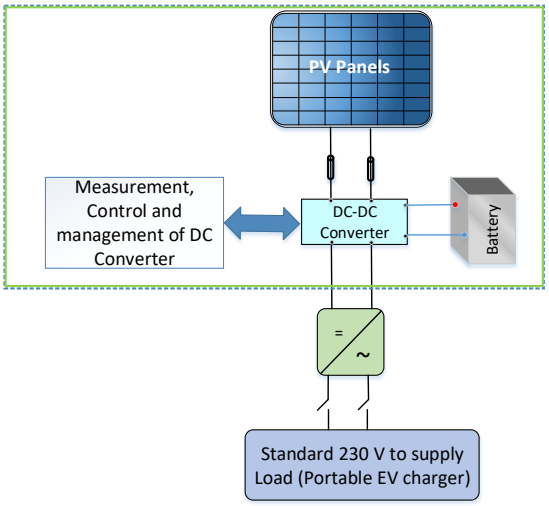


Figure 1. Block diagram of system configuration

### 2.1. Sizing and specifications of PV system

The PV powered EV charging system is designed to serve the employees and students attending the Applied Science Private University. Therefore, the sizing and design of the PV powered parking system for EV is designed with the following constraints:

- The university operating time from 8.00 AM to 5.00 PM.
- The space does not exceed the maximum area of 2 parking lots of around 36 $m^2$.
- The PV powered car parking system provides sufficient charging for EV for a minimum driving range of 30-40 km within the capital city during the operating time.
- The system to operate in off grid supported with battery pack to provide at least one day of autonomy.

The first constraint is related to the time during which the users may need to recharge their EVs. Also, this condition specifies the main time during which the solar irradiance is available to supply energy to the load. The measurements, as in Figure 2, were taken daily between 10.00 AM and 05.00 PM over a duration of one year, i.e., the period from January to December 2022, at the test field station at the Applied Science Private University. The data showed that the average daily solar irradiance recorded the lowest value of approximately 2.5 kWh during the month of December.

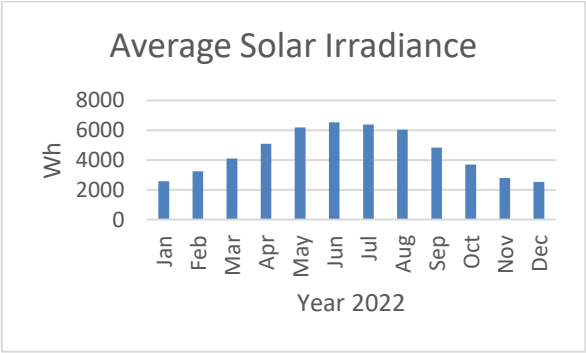


Figure 2. Monthly average solar irradiance received daily between 10:00 am and 5:00 pm at ASU field test station

Design for the worst month shows that the month of December has the lowest solar irradiance of 2.5 kWh or a PSH of 2.5. If the daily energy requirement is taken as 8 kWh for 40 km based on the data given in [7]. Hence, the equation that may be used to size a stand-alone PV system is [23]:

$$W_{PV} = \frac{E}{PSH \times \eta_{sys}} \quad (1)$$

Where, $W_{PV}$ is the peak wattage of the array in Wp, $E$ is daily energy requirements in Wh, $PSH$ is the average daily number of PSHs in the design month for the inclination and orientation of the PV array, and $\eta_{sys}$ is the total system efficiency.

Hence using (1) the PV panels are required to give $W_{PV} \approx 5\ kWp$ considering an overall system efficiency of 70%. Metaye [24] Renogy's monocrystalline solar panels are high-powered 550-watt solar panels made with half-cell technology. This half-cut panel is more tolerant of shading on any part of the cell and performs excellently in low light situations due to the increased number of cells receiving more sunlight. The space requirement for producing $5\ kWp$ may not exceed $23.5\ m^2$.

### 2.2. Sizing of storage battery

Deep cycle batteries are generally used in solar PV systems and are especially designed for the type of charging and discharging cycles they need to endure. These batteries can be characterized (in addition to their ability to be recharged) by high power density, high discharge rate, flat discharge curves, and good low-temperature performance. Deep cycle batteries are designed to be repeatedly charged and discharged all the way down to a very low charge, by as much as 80% of their full capacity without sustaining any serious damage to the cells. Normally, the range of the SOC is from 20% to 95% [21].

The battery is required to store energy for many days and to be used without going over the maximum depth of discharge ($DOD_{max}$). The minimum battery capacity required can be determined using (2) as given in [23]:

$$Q = \frac{E \times A}{V \times T \times \eta_{inv} \times \eta_{sys}} \quad (2)$$

where $Q$ is the minimum battery capacity required in Ah, $E$ is the daily energy requirement in Wh (8 kWh), $A$ is the number of days of storage required (1 day), $V$ is the system DC voltage ($V = 24\ V$), $T$ is the maximum allowed DOD of the battery usually on battery data sheet (indicatively 0.2-0.95), $\eta_{inv}$ is the inverter efficiency (1,0 if there's no inverter), and $\eta_{sys}$ is the efficiency of the cables delivering the power from battery to loads (0.8).

The size of the battery is selected to be sufficient to allow the system for one day of autonomy (daily requirement of 8 kWh) as specified above. Taking into consideration the system losses and battery efficiency, the size of the battery is chosen to 8 kWh, 24 V, deep cycle battery with depth of discharge up to 80%, hence using in (2), the battery capacity (Ah) is selected to be in the range of 520 Ah.

### 2.3. Design of DC-DC converter

The PV panels will supply their output of 48V to a DC-DC converter that is required to operate in step up (boost) mode to supply around 72 V to the DC bus that feeds a single-phase inverter which in turn will produce the standard 230 V AC as the plug for charging EV battery. On the other hand, when the PV output power is below the minimum requirements, the EV load is supplied by the 24 V battery pack. Finally, when the EV load is not connected, the PV panels will charge the storage battery through a buck converter if the SOC of the storage battery is below the predetermined level. Table 1 shows the operating modes of the DC-DC converter and the input/ output voltages for each operating mode.

Table 1. Operating modes of DC-DC converter

| Input type | Output load | Nominal duty cycle | Mode of operation |
|---|---|---|---|
| PV system 48 V | EV load (inverter 72 V) | 0.33 | Mode 1: step up |
| Storage battery 24 V | EV load (inverter 72 V) | 0.67 | Mode 2: step up |
| PV system 48 V | Storage battery 24 V | 0.50 | Mode 3: step down |

Figure 3 shows the general layout of the boost circuit used for modes 1 and 2. The following section explains the sizing of the DC-DC converter components for boost modes of operation.

a. Boost operation

The load is assumed to be 5 kW with the output voltage is set to 70.7 V, this will result in an output current of 70.7 A, equivalent to a load of ($R_l = 1.0\ \Omega$). The step-up converter will operate at a (minimum) duty cycle of 0.33 when the load is supplied by the PV system, and at a (maximum) duty cycle of 0.67 when the battery is discharged to supply the load. Limits are also set for the converter to operate in continuous conduction mode (CCM) when supplied by either source (PV or battery), and to strictly limit the input current ripple (inductor ripple current) not to exceed 40% with output voltage ripple less than 1%.

The nominal inductor current $I_L = 70.7\ A$, thus $\Delta I = 28.3\ A$ when the input voltage is 48 V. Similarly, when the input voltage is 24 V, the inductor current $I_L = 141.4\ A$, thus $\Delta I = 56.6\ A$. In (3) is used to design the filter inductor to fulfill the above requirements as in (3) [25].

$$L_1 \geq \frac{V_S \times D}{\Delta I \times f_S} = \frac{48 \times 0.33}{28.3 \times 10000} = 56\ \mu H$$

$$L_1 \geq \frac{V_S \times D}{\Delta I \times f_S} = \frac{24 \times 0.67}{56.6 \times 10000} = 28.4\ \mu H \quad (3)$$

Thus, $L_2$ is selected to be $100\ \mu H$ larger than the largest value of the above two, to ensure that the boost converter will adhere to the limits above when operated by either source. The ripple in the output voltage is limited to 1% (for design of C, output capacitor). For the converter when supplied by the battery, it operates at a duty cycle of 0.67, hence the size of the capacitor C,

$$C_1 \geq \frac{D}{R_l \times f_S \times (\Delta V/V)} = \frac{0.67}{1.0 \times 10000 \times 0.01} = 6700\ \mu F \quad (4)$$

Similarly, for the duty ratio of 0.33 when the converter is supplied by the PV source, the size of the capacitor C,

$$C_1 \geq \frac{D}{R_l \times f_S \times (\Delta V/V)} = \frac{0.33}{1.0 \times 10000 \times 0.01} = 3300\ \mu F \quad (5)$$

Again, the capacitance of the filter capacitor, $C_1$, is selected to be larger than the largest value of the above two values to ensure that the boost converter will adhere to the limits above when operated by either source.

b. Buck operation

When the EV load is not connected, a step down (buck) converter is operated to charge the 24 V battery pack. For the buck operation, the 5 kWp 48 V PV system is used for charging the 8 kWh, 24 V storage battery. If it is assumed that the PV system is subjected to full irradiance of 1000 W/m$^2$, then neglecting the losses the PV system will take approximately 2 hours to fully charge the storage battery. The charging time is well below the worst month PSH (2.5), which considers system efficiency of 70%. Therefore, the buck converter is designed to be capable of receiving a maximum current of 100 A ($I_{PV} = \frac{5\ kW}{48}$) as an input. Figure 4 shows the general circuit topology used for the buck operation mode. The ripple in the inductor current is limited to 30%, hence the value of the inductor $L_1$ is determined as in (6):

$$L_1 \geq \frac{V_{pv}}{4 \times \Delta I \times f_S} = L_2 \geq \frac{48\ v}{4 \times 3 \times 10 kHz} = 0.4\ mH \quad (6)$$

For the ripple in the output voltage,

$$C_2 \geq \frac{(1-D)}{8 \times L \times (\Delta V/V) \times f_S^2} = C_2 \geq \frac{0.5}{8 \times 0.4 \times 10^{-3} \times 0.01 \times 10^8} = 156\ \mu F \quad (7)$$

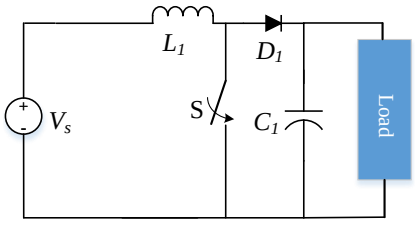


Figure 3. DC-DC converter boost operation

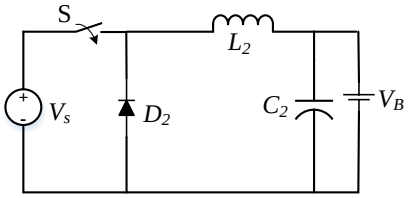


Figure 4. DC-DC converter buck operation

### 2.4. Proposed controller design

Three PI controllers were designed to control the operation of the DC-DC converters to track the MPP operation and maximize the efficiency of the PV charging system. The P&O algorithm is used to set the operating point for the DC-DC converter for modes 1 and 2 to track the MPP operation of the PV system. The control system implements three scheduled sets of gains ($K_p$ *and* $K_i$) for PI controllers to support the buck and boost modes of operation, thus generating the reference signals for the PWM controller which drives the DC-DC converter. Figures 5(a) to (c) shows the general structure of the three controllers used in the three modes of operation.

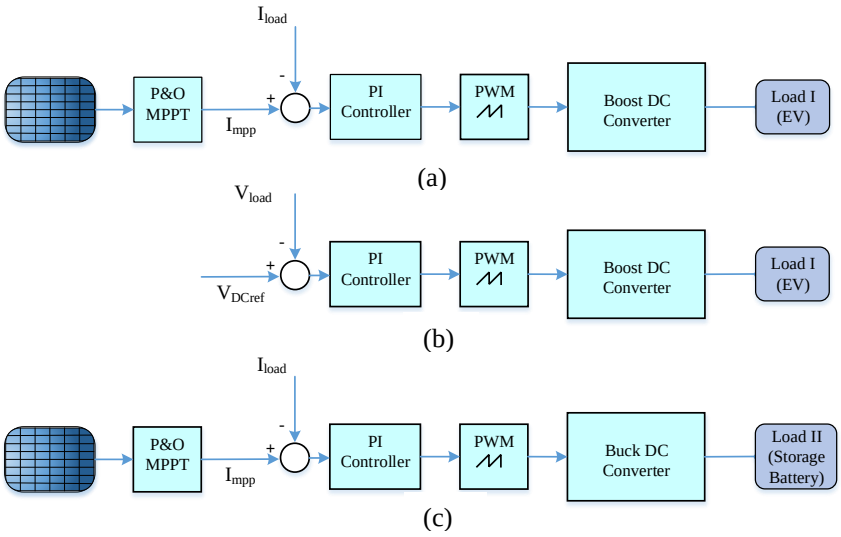


Figure 5. DC-DC converter control system; (a) mode I: PV supplying EV load boost operation, (b) mode II: storage battery supplying EV load boost operation, and (c) mode III: PV charging storage battery buck operation

The topology for the DC-DC converter in Figure 3 is used to develop the state space average model when operating in modes I and II based on the concept presented in [26]. The transfer function for boost operation in mode I:

$$\frac{\Delta I_o(s)}{\Delta D(s)} = \frac{-0.03285\, s^2 - 7109\, s + 3.51\times10^7}{s^2 + 252.7\, s + 2.609\times10^5} \quad (8)$$

Transfer function for battery supplying the load in mode II:

$$\frac{\Delta V_o(s)}{\Delta D(s)} = \frac{-0.04862\, s^2 - 1.052\times10^4\, s + 5.195\times10^7}{s^2 + 252.7\, s + 2.609\times10^5} \quad (9)$$

Transfer function for buck operation mode III:

$$\frac{\Delta I_b(s)}{\Delta D(s)} = Y(s)_{buck} = \frac{3.284\times10^4\, s + 5.469\times10^{10}}{s^2 + 1.582\times10^5\, s + 1.046\times10^9} \quad (10)$$

The proportional and integral gains of the PI controllers for the three modes of operation are tuned using the corresponding transfer function for each mode and the PI controller tuning facility available from MATLAB.

### 2.5. Management of operating modes

Figure 6 shows the complete circuit diagram of the proposed converter topology for the three operating modes. Switches $S_1, S_2, and\ S_3$ are operated as ON and OFF switching devices to select the operating mode of the circuit. On the other hand, switches $S_4\ and\ S_5$ are operated as PWM switching devices to control the operation of the converter while in the selected mode. Table 2 shows the state of each switch for each of the three modes of operation.

The selection of the operating mode is determined using the flowchart in Figure 7. The system checks first if the load switch is ON (i.e., EV is plugged to the system), if yes then it proceeds to check if the PV panels have enough available power (above 50% of rated power) to charge the EV. If the PV doesn't have enough power the system will examine if the SOC of the storage is above 40%, it will then supply the EV load through the discharge of the storage battery. The 40% SOC limit is set to avoid discharging the storage battery below acceptable limits. For the case when the EV load is not connected the PV panels are used to charge the storage battery if the SOC is below 90%. The limit not to charge the storage battery above 90% is set to avoid overcharging and extend the lifetime of the battery.

An event driven FSM is designed to implement the switching logic that manages the operating modes of the EV charging system based on the flowchart in Figure 7. To avoid overlapping of the switching between operating modes and hence to prevent any short circuit conditions, the FSM is directed to the initial state when switching between states. Figure 8 shows the state diagram of the FSM and a simple NAND logic implementation.

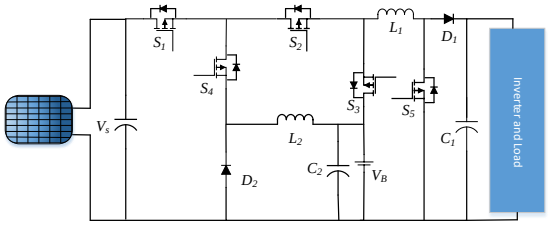


Figure 6. DC-DC converter circuit topology

Table 2. State of Switches corresponding to the operating modes

| $S_1$ | $S_2$ | $S_3$ | $S_4$ | $S_5$ | Mode | Notes |
|---|---|---|---|---|---|---|
| ON | ON | OFF | OFF | SW | Mode I: boost | PV source $V_s$ is supplying the load and $S_5$ is switching transistor. |
| ON | OFF | OFF | SW | OFF | Mode II: buck | PV source $V_s$ is charging the battery and $S_4$ is switching transistor. |
| OFF | OFF | ON | OFF | SW | Mode III: boost | Battery $V_B$ is discharging and $S_5$ is switching transistor. |

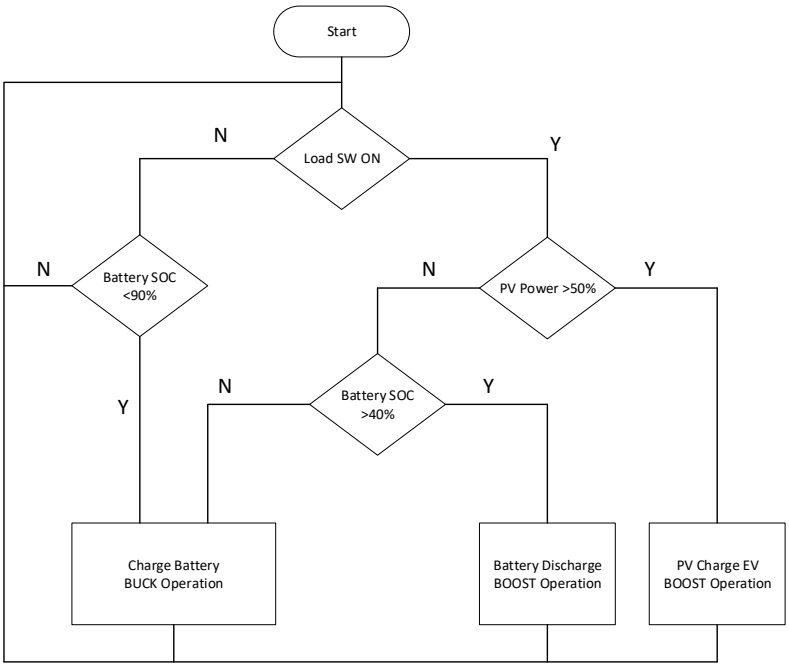


Figure 7. Operating modes flowchart

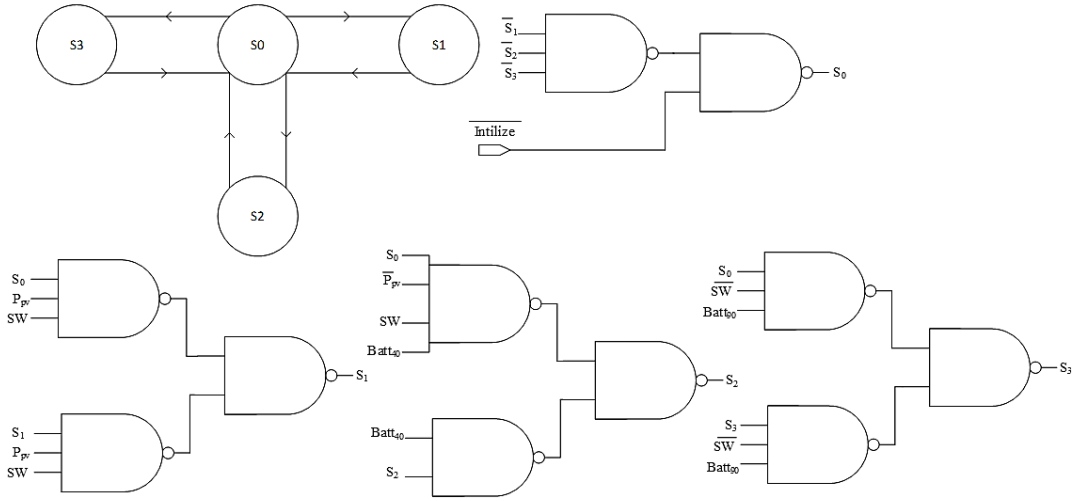


Figure 8. State diagram and NAND logic implementation

## 3. SIMULATION RESULTS AND DISCUSSION

The proposed system is examined by simulation using Simulink/MATLAB. Initial settings of the system assumed that system is required to track the MPP when the PV system is supplying either the EV load (mode I) or charging the storage battery (mode III). For the case when the converter is operating in mode I to supply power to EV load, a single-phase controlled inverter stage followed by a step-up transformer are required to produce the standard AC outlet voltage of 230 V. The transformer turns ratio is specified based on the lowest level of solar irradiance as specified by the system ($500\ W/m^2$). Since the output voltage from the DC converter will be varying flowing the MPP tracking to allow the extraction of the maximum available power from the PV panel, the inverter firing angle must be adjusted to maintain the standard 230 V output voltage. The results of the DC converter when operating in the three modes are discussed in the following sections.

### 3.1. Management of system operation

The management of the system is examined first as in Figure 9. The system will remain in the initial state $s_0$ until t=2 s, although the load is connected at t=1 s since both PV system and storage battery don't meet the minimum threshold to supply the load. At time t=2 s, the battery SOC is above 40%, hence the load will be supplied by discharging the battery as in state $s_2$. The system will remain in state $s_2$ until the time t=5 s when the battery SOC drops below 40%. The load will then be supplied by the PV system since it has its available power above the threshold of 50%, hence state $s_1$ will be triggered from t=5s until t=7s when the load is disconnected. From t=7s, the PV panels will charge the storage battery since the SOC is found below 90%.

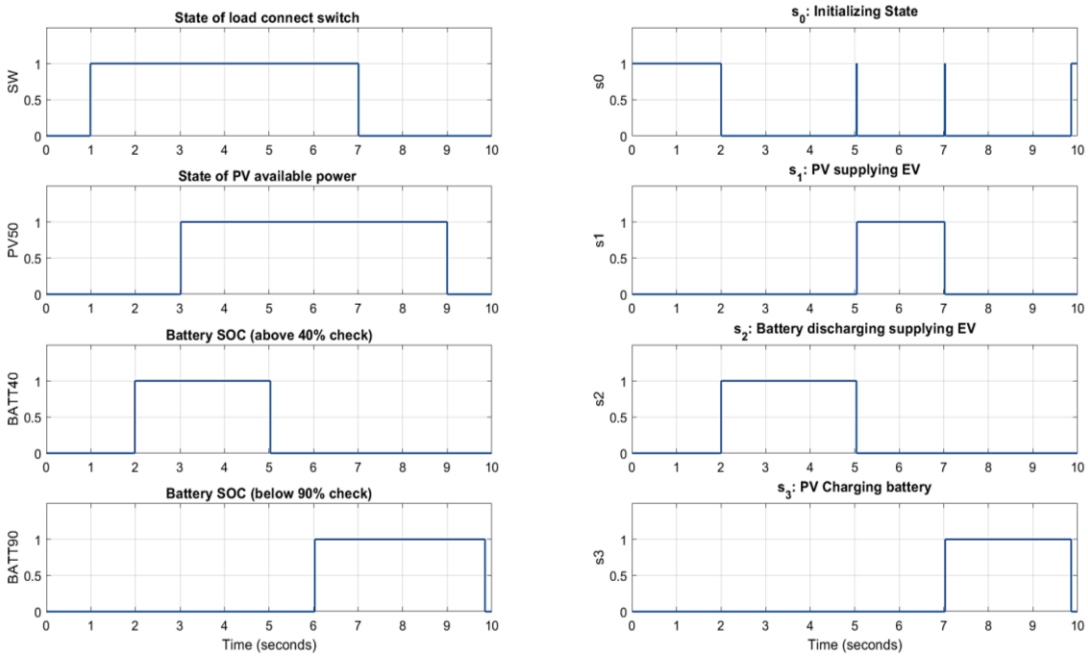


Figure 9. Operating modes control signals

### 3.2. Mode I: boost operation PV charging EV load

In this setup the system is examined under constant temperature of 25 ºC with varying irradiance between 1000 and 500 W/m$^2$. Figure 10 shows the simulation results for mode I, with the converter supplying a load equivalent to 1 Ω with a step and ramp change in the solar irradiance. It can be seen from Figure 10 that the power supplied to the load can track the maximum power available from the PV panels. The output power maintained its value by supplying the maximum power at time $t = 6\ s$ when the load is increased by 10% by dropping the load from 1 Ω to 0.9 Ω, with the solar irradiance maintained at 1000 W/m$^2$. To study the temperature effect on the system, the same setup for mode I above is used but this time the solar irradiance is maintained constant at 1000 W/m$^2$ with the temperature varied in step change from 15 to 39 ℃ as shown in Figure 11. The converter system showed good performance in tracking the variation in the maximum power produced by PV panels due to the temperature variation.

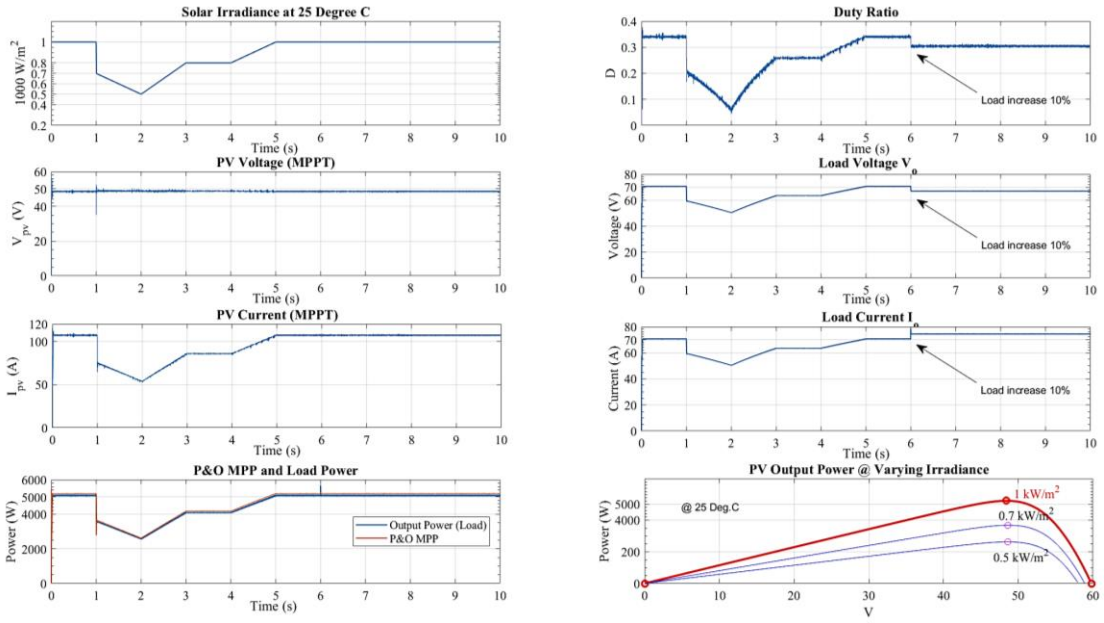


Figure 10. Operation in mode I, converter supplies power to load under varying solar irradiance and constant temperature

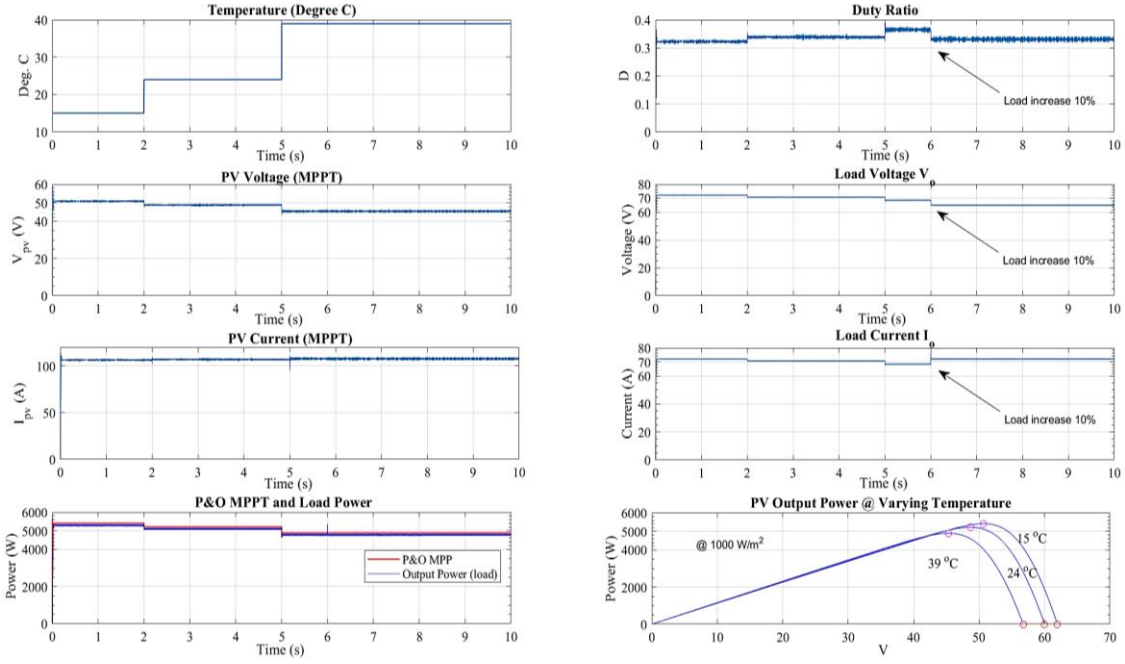


Figure 11. Operation in mode I, converter supplies power to load under constant solar irradiance and varying temperature

### 3.3. Mode II: battery supplying load

Figure 12 shows the simulation results when the PV panels are not receiving enough solar irradiance and the load is supplied by the storage battery and the system was capable of switching to supply the load from the storage battery. The battery SOC is set to 40% with the converter supplying a load equivalent to 1 Ω. In this mode the converter maintained the load output voltage at 70.7 V since the MPP tracking is no longer needed as the input source is the storage battery. At time $t = 3\ s$ the load is increased by 10% by dropping the load from 1 Ω to 0.9 Ω, as a result the output voltage maintained its value at around 70.7 V while the output current is increased to maintain a constant power supply to load.

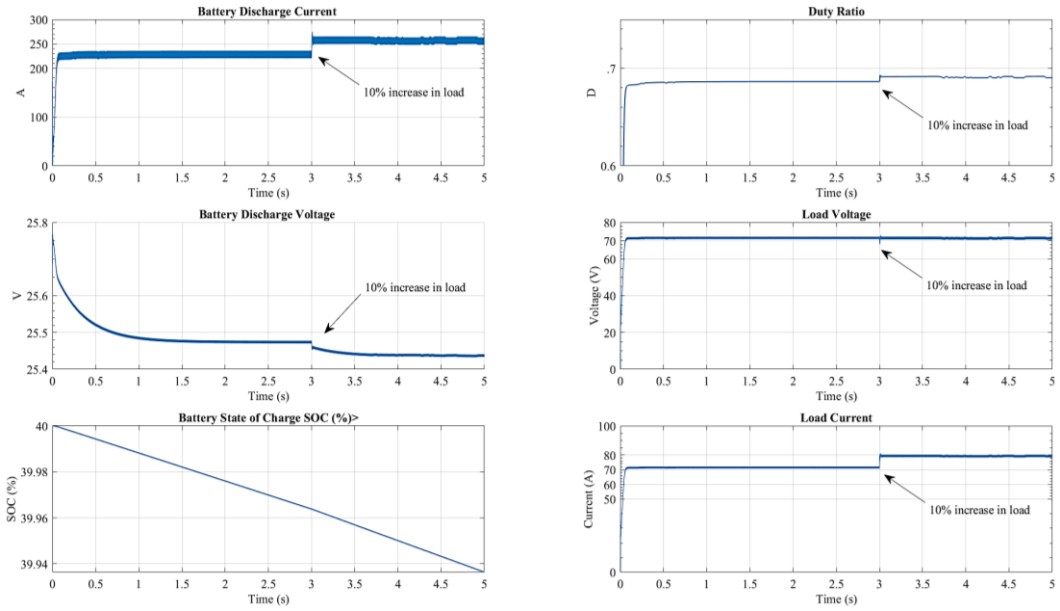


Figure 12. Operation in mode II, battery discharging power to load with battery SOC at 40%

### 3.4. Mode III: buck operation PV charging storage battery

The buck operation of the converter is examined in this section. Figure 13 shows the operation of the system under varying solar irradiance with EV load is disconnected. The converter is used to charge the storage battery if its SOC is below 90%. The P&O algorithm is used to extract maximum power from PV system to charge the storage battery. As Figure 13 shows, the PV output power varies according to the variation in the solar irradiance, and hence the estimated PV power using the P&O method. Also, the converter showed good tracking performance by changing the power supplied to the load (to charge the storage battery). In this mode of operation, the PV output voltage is stepped down using the buck converter to charge the battery at around 26.0 volts.

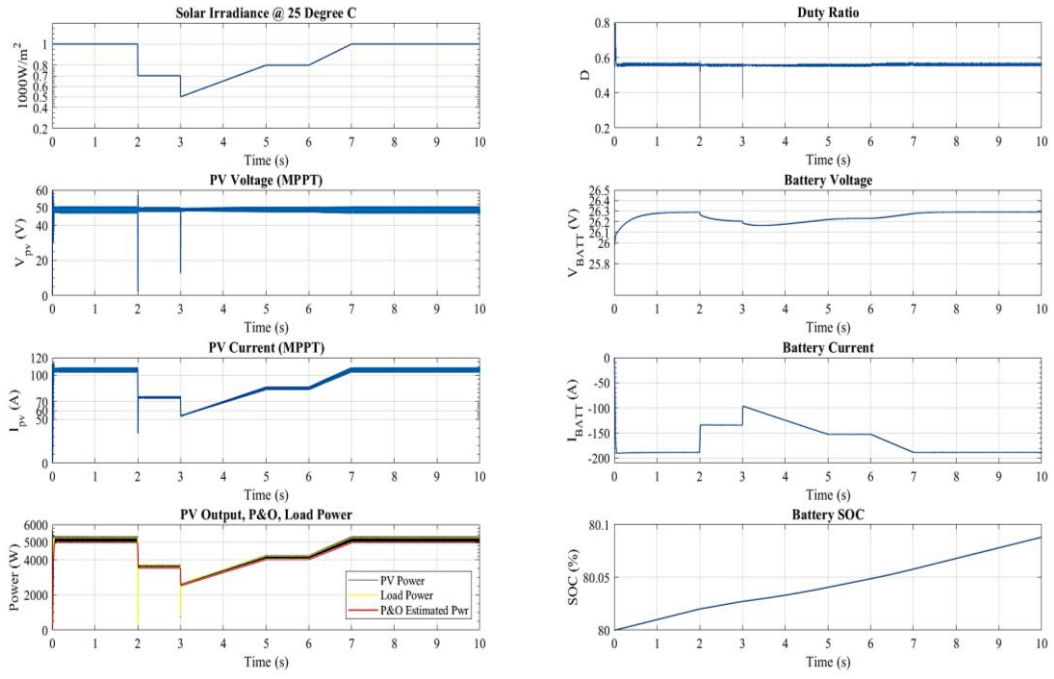


Figure 13. Operation in mode III, converter charging the battery

## 4. CONCLUSION

This paper presented direct charging of EV using standalone PV panels that cover carparking at workplace. The solution presented in this paper presents a sustainable source for EV charging, and it also serves the purpose of providing shade or protection from the sun during the summer season. The system is sized and designed using the worst PSH from the data available from the average solar irradiance received at the Applied Science Private University in Amman. The sizing and design of the system took into consideration one day of autonomy to supply power during cloudy days. Three modes of operation for the car park charging system are organized using a simple event driven FSM. The PV system is designed to utilize the maximum available energy from the solar panels using the P&O method. The proposed system showed good tracking functionality to adjust the system's operating point according to the MPP using PI controllers.

## REFERENCES


[1] International Energy Agency (IEA), "Global EV Outlook 2023 - Catching up with climate ambitions," *Global EV Outlook 2023*, no. Geo, pp. 9–10, 2023, [Online]. Available: https://www.iea.org/reports/global-ev-outlook-2023. (accessed 1 Sep 2023).

[2] M. Wiatros-Motyka *et al.*, "Krzysztof Bolesta (European Commision), Toby Lockwood (Clean Air Task Force), Lauri Myllyvirta," pp. 1–163, 2023.

[3] K. S. P. Oruganti, C. A. Vaithilingam, G. Rajendran, and A. Ramasamy, "Design and sizing of mobile solar photovoltaic power plant to support rapid charging for electric vehicles," *Energies*, vol. 12, no. 18, p. 3579, Sep. 2019, doi: 10.3390/en12183579.

[4] A. A. Naqvi, T. Bin Nadeem, A. Ahmed, and A. A. Zaidi, "Designing of an off-grid Photovoltaic system with battery storage for remote location," *Tecciencia*, vol. 16, no. 31, pp. 15–28, Dec. 2021, doi: 10.18180/tecciencia.2021.31.2.

[5] A. Singh, S. S. Shaha, P. G. Nikhil, Y. R. Sekhar, S. Saboor, and A. Ghosh, "Design and analysis of a solar-powered electric vehicle charging station for Indian cities," *World Electric Vehicle Journal*, vol. 12, no. 3, p. 132, Aug. 2021, doi: 10.3390/wevj12030132.

[6] S. M. Shariff, M. S. Alam, F. Ahmad, Y. Rafat, M. S. J. Asghar, and S. Khan, "System Design and Realization of a Solar-Powered Electric Vehicle Charging Station," *IEEE Systems Journal*, vol. 14, no. 2, pp. 2748–2758, Jun. 2020, doi: 10.1109/JSYST.2019.2931880.

[7] G. R. C. Mouli, P. Bauer, and M. Zeman, "System design for a solar powered electric vehicle charging station for workplaces," *Applied Energy*, vol. 168, pp. 434–443, Apr. 2016, doi: 10.1016/j.apenergy.2016.01.110.

[8] T. Taufik, T. Wong, O. Jong, and D. Dolan, "Design and simulation of multiple-input single-output DC-DC converter," in *Proceedings of the 9th International Conference on Information Technology, ITNG 2012*, Apr. 2012, pp. 478–483, doi: 10.1109/ITNG.2012.109.

[9] M. A. Rosli, N. Z. Yahaya, and Z. Baharudin, "Multi-input DC-AC Inverter for Hybrid Renewable Energy Power System," *International Journal of Electrical and Computer Engineering (IJECE)*, vol. 6, no. 1, p. 40, Feb. 2016, doi: 10.11591/ijece.v6i1.8718.

[10] S. K. Haghighian, S. Tohidi, M. R. Feyzi, and M. Sabahi, "Design and analysis of a novel SEPIC-based multi-input DC/DC converter," *IET Power Electronics*, vol. 10, no. 12, pp. 1393–1402, Oct. 2017, doi: 10.1049/iet-pel.2016.0654.

[11] C. Anuradha, N. Chellammal, M. S. Maqsood, and S. Vijayalakshmi, "Design and analysis of non-isolated three-port SEPIC converter for integrating renewable energy sources," *Energies*, vol. 12, no. 2, p. 221, Jan. 2019, doi: 10.3390/en12020221.

[12] D. F. Al Riza and S. I. U. H. Gilani, "Standalone photovoltaic system sizing using peak sun hour method and evaluation by TRNSYS simulation," *International Journal of Renewable Energy Research*, vol. 4, no. 1, pp. 109–114, 2014.

[13] P. Viveros, F. Wulff, F. Kristjanpoller, C. Nikulin, and T. Grubessich, "Sizing of a Standalone PV System with Battery Storage for a Dairy: A Case Study from Chile," *Complexity*, vol. 2020, pp. 1–17, Dec. 2020, doi: 10.1155/2020/5792782.

[14] A. H. El Khateb, N. A. Rahim, and J. Selvaraj, "Fuzzy Logic Control Approach of a Maximum Power Point Employing SEPIC Converter for Standalone Photovoltaic System," *Procedia Environmental Sciences*, vol. 17, pp. 529–536, 2013, doi: 10.1016/j.proenv.2013.02.068.

[15] M. Awad, A. M. Ibrahim, Z. M. Alaas, A. El-Shahat, and A. I. Omar, "Design and analysis of an efficient photovoltaic energy-powered electric vehicle charging station using perturb and observe MPPT algorithm," *Frontiers in Energy Research*, vol. 10, Aug. 2022, doi: 10.3389/fenrg.2022.969482.

[16] A. Affam, Y. M. Buswig, A.-K. B. H. Othman, N. Bin Julai, and O. Qays, "A review of multiple input DC-DC converter topologies linked with hybrid electric vehicles and renewable energy systems," *Renewable and Sustainable Energy Reviews*, vol. 135, p. 110186, Jan. 2021, doi: 10.1016/j.rser.2020.110186.

[17] A. E. F. A. Omran, A. E. S. A. Nafeh, and H. K. M. Yousef, "Optimal Sizing of a PV-Battery Stand-Alone Fast Charging Station for Electric Vehicles Using SO," *International Journal of Renewable Energy Research*, vol. 12, no. 4, pp. 1769–1788, 2022, doi: 10.20508/ijrer.v12i4.13487.g8602.

[18] D. K. Nair, K. Prasad, and T. T. Lie, "Design of a PV-fed electric vehicle charging station with a combination of droop and master-slave control strategy," *Energy Storage*, vol. 5, no. 5, Aug. 2023, doi: 10.1002/est2.442.

[19] R. Ragul, N. Shanmugasundaram, M. Paramasivam, S. Seetharaman, and S. L. M. Immaculate, "PV Based Standalone DC -Micro Grid System for EV Charging Station with New GWO-ANFIS MPPTs under Partial Shading Conditions," *International Transactions on Electrical Energy Systems*, vol. 2023, pp. 1–14, Mar. 2023, doi: 10.1155/2023/2073742.

[20] B. R. Putri, I. Sudiharto, I. Ferdiansyah, A. B. Karso, and D. S. Yanaratri, "Design SEPIC Converter for Battery Charging Using Solar Panel," *Journal of Physics: Conference Series*, vol. 1844, no. 1, p. 012015, Mar. 2021, doi: 10.1088/1742-6596/1844/1/012015.

[21] I. E. Atawi, E. Hendawi, and S. A. Zaid, "Analysis and design of a standalone electric vehicle charging station supplied by photovoltaic energy," *Processes*, vol. 9, no. 7, p. 1246, Jul. 2021, doi: 10.3390/pr9071246.

[22] M. Brenna, F. Foiadelli, C. Leone, and M. Longo, "Electric Vehicles Charging Technology Review and Optimal Size Estimation," *Journal of Electrical Engineering and Technology*, vol. 15, no. 6, pp. 2539–2552, Nov. 2020, doi: 10.1007/s42835-020-00547-x.

[23] A. Bhatia, "Design and Sizing of Solar Photovoltaic Systems Credit," *CEDengineering*, no. 877, pp. 37–42, 2022.

[24] R. Metaye, "1 kW Solar Panel (Ultimate Guide to A 1 kW Solar System)," 2022, [Online]. Available: *Https://Climatebiz.Com/1Kw-Solar-Panel/*, 2022. (accessed 2 Apr 2021).

[25] D. W. Hart, *Power Electronics*, 1st ed. Tata McGraw-Hill, 2011.
[26] W. M. Polivka, P. R. K. Chetty, and R. D. Middlebrook, "State-Space Average modelling of converters with parasitics and storage-time modulation," in *PESC Record - IEEE Annual Power Electronics Specialists Conference*, vol. 1980, pp. 119–143, Jun. 1980, doi: 10.1109/PESC.1980.7089440.

## BIOGRAPHIES OF AUTHORS

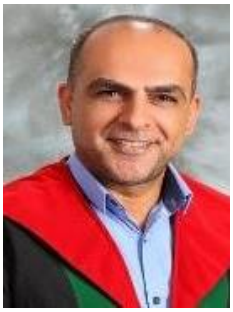

**Eyad Radwan** completed his B.Sc. from JUST 1996, M.Sc. and Ph.D. from UPM (Malaysia) in 1999 and 2004 respectively. From 1999 to 2011 he was with UCSI University and served as the Dean of the Faculty of Engineering and Built Environment from 2007 to 2009, and as Chief Operating Officer from 2009 to 2011. He joined the department of electrical engineering at the Applied Science Private University, Jordan in 2012. His specialization is in the area of electrical power and renewable energy, drives, and control. He can be contacted at email: e_redwan@asu.edu.jo.

**Emad Awada** received his B.S. in Electrical Engineering from Prairie View Texas A&M University (PVAMU) in 1998. He also, received his M.S. and Ph.D. in Electrical Engineering, PVAMU 2006 and 2011 respectively. His work experiences were in the field of electrical power, energy, and signalprocessing. His research interests are in the areas of power system, renewable energy, energy conservation, mixed signals systems, signal processing, and power fault detection. Currently, he is a full-time at Al-Balqa Applied University, Department of Electrical Engineering. He can be contacted at email: emad.awada@bau.edu.jo.

**Mutasim Nour** is the Associate Director of External Relations and Industry Engagement in the School of Engineering and Physical Sciences at Dubai Campus and a member of IEEE and JEA. He is also the Director of studies for M.Sc. Energy and Renewable Energy Engineering programmers at the Dubai Campus. Before joining Heriot-Watt University, he was an Associate Professor at the University of Nottingham Malaysia Campus. He can be contacted at email: mutasim.nour@hw.ac.uk.